Journal of the Serbian Chemical Society
JSCS-info@shd.org.rs • www.shd.org.rs/JSCS
J. Serb. Chem. Soc. *89* (6) 877–890 (2024)
JSCS–5761
Original scientific paper
Published 30 June 2024

Investigation of structural, dynamic and dielectric properties of an aqueous potassium fluoride system at various concentrations by molecular dynamics simulations

AYOUB LAHMIDI, SANAA RABII, ABDELKBIR ERROUGUI*, SAMIR CHTITA, MHAMMED EL KOUALI and MOHAMMED TALBI

Laboratory of Analytical and Molecular Chemistry, Faculty of Sciences Ben M'Sick, Hassan II University of Casablanca, Morocco

(Received 6 November, revised 23 December 2023, accepted 19 January 2024)

Abstract: Potassium-ion-based batteries have emerged as promising alternatives to traditional lithium-ion batteries for energy storage systems due to their affordability, wide accessibility and comparable chemical characteristics to lithium. This study employs molecular dynamics simulations to explore the physical phenomena of potassium fluoride in aqueous solutions. The interatomic interactions were defined using the OPLS-AA force field, while the SPC/E water model and ions were represented as charged Lennard–Jones particles. The simulations were conducted across concentrations ranging from 0.1 to 1.0 mol kg^{-1}. The insights derived from this investigation provide valuable understanding into the behaviour of KF electrolytes and their potential utility in energy storage systems. A comprehensive comprehension of the impact of KF electrolyte concentration on structural, dynamic and dielectric properties is pivotal for the design and optimization of potassium-ion batteries, as well as other electrochemical devices leveraging KF-based electrolytes. This research significantly contributes to the ongoing endeavours aimed at developing efficient and economically viable energy storage solutions that transcend the confines of traditional lithium-ion batteries.

Keywords: molecular dynamics; potassium fluoride; hydration phenomenon; self-diffusion coefficient; dielectric constant; energy storage system.

INTRODUCTION

In recent years, a surge of interest has emerged in the pursuit of new battery technologies aimed at addressing the limitations of standard lithium-ion batteries.[1,2] One such promising development involves batteries centred around potassium ions, which hold potential as alternatives for energy storage systems.[3,4] These potassium-ion batteries offer several advantages over their lithium-ion

* Corresponding author. E-mail: Abdelkbir.errougui@univh2c.ma
https://doi.org/10.2298/JSC231106003L

counterparts, including reduced costs, abundant availability and comparable chemical properties.[5–7]

Lithium-ion batteries have become the preferred choice across various applications, ranging from portable devices to electric automobiles.[8,9] However, their production costs remain relatively high due to limited global lithium reserves and intricate extraction processes.[10,11] Furthermore, lithium-ion batteries heavily rely on cobalt, a rare and costly material entangled with ethical and environmental concerns in its mining.[12,13] These factors have prompted researchers and scientists to explore alternative battery chemistries that can offer similar or enhanced performance while being more economically feasible and sustainable.

Significantly, potassium is an abundant element present in the Earth's crust and readily available, rendering it a cost-effective substitute for lithium.[14,15] Its widespread availability ensures a steady and sustainable supply chain, reducing the concerns related to resource scarcity.[7] Additionally, the potassium ions exhibit comparable chemical properties to lithium ions, enabling them to demonstrate akin electrochemical behaviour and energy storage capabilities.[16–18] Recent studies have exhibited promising results in the development of potassium-ion batteries.[19,20] Researchers have made substantial progress in augmenting battery performance, energy density, and cycle life, rendering these batteries more viable for practical applications.[21,22] These advancements primarily revolve around the design of suitable electrode materials, electrolyte formulations and battery architectures, all geared towards optimizing the performance and stability of the potassium-ion batteries.[23–25] Within various applications, particular attention has been directed towards the electrolytic system involving a fluoride anion and potassium cation due to its significance.[26–29] Nonetheless, a comprehensive examination of the existing literature uncovers a scarcity of molecular equilibrium simulation studies targeting $KF_{(aq)}$ systems within the specified concentration range.

The organization of this paper is as follows: Section 2 include the details for the MD simulations. Section 3 elucidates and presents the theoretical equations employed in this investigation. Section 4 deals with the study's findings, including computed structural and dynamical characteristics, alongside the dielectric constant at different concentrations. Lastly, Section 5 summarizes the conclusions and concluding remarks.

COMPUTATIONAL DETAILS

In this research, we conducted molecular dynamics (MD) simulations at a temperature of 298.15 K to investigate the behaviour of potassium fluoride (KF) within aqueous solutions of varying concentrations. To describe the interatomic potentials between ions and water components,[30] we employed the optimized potentials for liquid simulations-all atom (OPLS-AA) force field. The simulations were carried out using GROMACS-2020-6[31,32] under the NPT ensemble, wherein both particle number (N) and pressure were held constant at 1 bar using

Parrinello–Rahman pressure coupling.[33] To maintain the temperature at 298.15 K, a Nosé––Hoover thermostat was used.[34,35]

The simulations were carried out for a total of 10^8 steps, with each time step set to 0.1 fs, resulting in a simulation time of 100 ns. This extended simulation time allowed for a comprehensive exploration of the system's dynamics and behaviour. For representing water molecules, we employed the widely used SPC/E model,[36] known for its accuracy in reproducing numerous solution properties.

The interaction between ions and water molecules was depicted through Coulombic interactions and a short-range Lennard–Jones (LJ) potential,[37] with the ions interacting selectively with oxygen or hydrogen atoms within the water molecules, Table I. The main aim of this study is to gain insights into the behaviour and properties of potassium fluoride within an aqueous solution. Through our simulations we computed the radial distribution functions (RDFs) for different ion pairs, uncovering the microstructural characteristics of the solutions. Furthermore, we determined the hydration numbers by integrating the RDFs. Additionally, we evaluated the dynamic and dielectric properties of different components by modelling the self-diffusion coefficient and relative permittivity (ε). These simulations provided a comprehensive understanding of the interatomic interactions and dynamics within the system, shedding light on the structural, dynamical and dielectric properties of the potassium fluoride solution.

TABLE I. Lennard–Jones interactions and electrostatic forces parameters within the force fields of water and ions[38,39]

Element	q / e	σ_{LJ} / Å	ε_{LJ} / kcal* mol^{-1}
K^+	1.00000	4.93463	0.00033
F^-	–1.00000	2.73295	0.72000
O_w	–0.84760	3.16560	0.65017
H_w	0.42380	3.16549	0.15532

Theoretical formalism

In this system, both the interactions between ions {ion–ion} and ions with dipoles {ion––dipole} are modelled using a combination of Coulombic and Lennard–Jones potentials. The general representation of the potential is :[40]

$$U_{ij}(r) = \frac{q_i q_j}{r_{ij}} + 4\varepsilon_{ij}[(\frac{\sigma_{ij}}{r_{ij}})^{12} - (\frac{\sigma_{ij}}{r_{ij}})^{6}] \quad (1)$$

The equation incorporates the charge of the the atom (or ion), denoted as q_i, and is essential in describing the Coulombic potential. Additionally, the Lennard–Jones parameters σ_{ij} and ε_{ij} are determined using the combination rules from Eqs. (2) and (3), respectively:

$$\sigma_{ij} = \frac{\sigma_i + \sigma_j}{2} \quad (2)$$

$$\varepsilon_{ij} = \sqrt{\varepsilon_i \varepsilon_j} \quad (3)$$

These combination rules play a pivotal role in the computation of the Lennard–Jones potential, responsible for describing the attractive and repulsive forces operating among particles. By employing this generalized potential equation, we attain invaluable insights into the intri-

* 1 kcal = 4184 J

cate interplay of forces within the system, thus contributing to a comprehensive grasp of its structural and dynamic behaviours.

For the analysis of structural properties within aqueous solutions, a crucial methodology involves the calculation of the radial distribution function (RDF), denoted as $g_{ij}(r)$, pertaining to various pairs of ions. Eq. (4) presented below encapsulates the mathematical representation of $g_{ij}(r)$ function, which characterizes the spatial distribution of ion pairs i and j. This equation quantifies the possibility of locating an ion i at a distance r_{ij} from ion j within the solution:[26,41]

$$g_{ij}(r) = 4\pi r^2 \rho \mathrm{d}r \tag{4}$$

To determine the coordination numbers, $n_{ij}(r)$, associated with different ions, we integrated the radial distribution function by:[41,42]

$$n_{ij}(r) = 4\rho_i \int_0^{r_{\min}} g_{ij}(r)\mathrm{d}r \tag{5}$$

This integration provides an estimation of the number of water molecules surrounding M^+ within the distance range from 0 to $r_{\min}$. Here, $g_{ij}(r)$ represents the RDFs for the i–j pair, while ρ_i denotes the number density of particles corresponding to the minimum of the first peak in the RDF. This analysis allowed us to gain insights into and quantify the extent of ion––water molecule interactions within the specific environment surrounding M^+ in the solution.

To characterize dynamic properties, our focus lies in computing the self-diffusion coefficient (D), a pivotal factor for representing the translational motion of particles within the aqueous system. This coefficient is determined by analysing the long-time limit of the mean square displacement (*MSD*) using Einstein's relation:[26]

$$D = \frac{1}{6}\lim_{t\to\infty}\frac{\mathrm{d}}{\mathrm{d}t}\frac{1}{N}\sum_{i=1}^{N}[|\, r(t_0+t) - r(t_0)\,|^2] \tag{6}$$

In Eq. (6), $r(t_0 + t)$ denotes the position vector of the molecule's (or ion's) centre of mass at time t. Through the analysis of the temporal evolution of the centre of mass position, we acquire enhanced insights into the diffusive patterns and motion of particles within the aqueous system.

Moreover, in the pursuit of deriving the dielectric constant of non-polarizable fluids, we evaluate the fluctuations in the total dipole moment (M) within the simulation volume. Eq. (7) provides the mathematical representation of this calculation:[26]

$$\varepsilon = \frac{4}{3K_{\mathrm{B}}T\langle V\rangle}(\langle M^2\rangle - \langle M\rangle^2) \tag{7}$$

Here, M represents the cumulative sum of individual dipole moments (μ_i) contributed by all particles in the system, where N denotes the total number of particles. The examination of these fluctuations furnishes significant insights into the dielectric characteristics of the non-polarizable fluid system, elucidating its electrical properties and interactions.

RESULTS AND DISCUSSION

Structural proprieties

The evolution of concentration within an electrolytic solution is a pivotal aspect for understanding the structural characteristics of complex systems, especially in the presence of an aqueous medium. However, upon analysing the litera-

ture, it has become evident that there exists a dearth of data concerning the influence of concentration on the $KF_{(aq)}$ system. Furthermore, this study leads us to the conclusion that the calculated density of these solutions exhibits a linear decrease as the concentration increases. To provide a comprehensive overview of the studied system, Table II presents our molecular simulation data, including parameters such as density, volume, number of hydrogen bonds, total energy, kinetic energy and structural properties of this system at various concentrations. The initial analysis aims to highlight the strong correlation between concentration and the examined physicochemical properties, thus enhancing our understanding of the dissolution process of potassium fluoride within an aqueous medium.

TABLE II. Simulation values reveals thermodynamic and structural properties of $KF_{(aq)}$ system at different concentrations

Parameter	C / mol kg^{-1}					Exp. data
	0.1	0.3	0.5	0.8	1.0	
ρ / 10^3 kg m^{-3}	1.005	1.011	1.032	1.053	1.067	–
V / nm^3	64.529	63.932	63.419	62.569	62.019	–
E_{tot} / 10^5 kJ mol^{-1}	–0.886	–0.951	–1.009	–1.107	–1.173	–
$E_{kinetic}$ / 10^5 kJ mol^{-1}	0.161	0.160	0.159	0.158	0.158	–
Number of H-bonds per H	1.677	1.702	1.724	1.765	1.793	–
$r_{(K\text{-}Ow)}$ / Å	2.720	2.720	2.720	2.720	2.720	2.80[43]
Hydration number ($_{CNK+}$)	6.602	6.634	6.665	6.708	6.735	6.40[44]
$r_{(F\text{-}Ow)}$ / Å	2.600	2.600	2.600	2.600	2.600	2.64[45]
Hydration number ($_{CNF-}$)	6.329	6.334	6.341	6.351	6.360	6.10[45]
						6.80[44]

To explore the local structure of the electrolyte system, we performed molecular dynamics simulations in a canonical NVT ensemble. This allowed us to calculate hydration data for all constituents, encompassing ions and water molecules. In particular, we scrutinized the pair correlations among ions, ion–water, and water–water interactions using radial distribution functions (RDFs). Our investigation centred on aqueous KF electrolytes maintained at a temperature of 298.15 K.

The RDFs, acquired across diverse concentrations spanning from 0.1 to 1.0 (mol kg^{-1}), have been obtained and are graphically depicted in Figs. 1–3. These RDF graphs offer valuable insights into the spatial arrangement and interplay between ions and water molecules within the KF electrolyte system. By analysing these RDFs, we gain enhanced comprehension of local structural attributes and their fluctuations with changing concentration levels. This research contributes to a more comprehensive understanding of the system's behaviour.

Radial distribution functions have yielded valuable insights into the microstructural properties of the electrolytic system in KF aqueous solution. Fig 1a illustrates the $g_{K–Ow}(r)$ first peak, which was detected at a distance of 0.272 nm,

indicating a well-defined coordination shell around the potassium cation. The second hydration shell was observed in the range of distance between 0.466 and 5.921 nm, suggesting the presence of additional water molecules in the environment. The $g_{F–Hw}(r)$ in Fig 1b exhibited dual peaks as well, with the initial peak observed at a separation of 0.159 nm, followed by a secondary peak at 0.305 nm. These findings are consistent with both experimental results and computer simulations conducted on the KF aqueous system.[43,45]

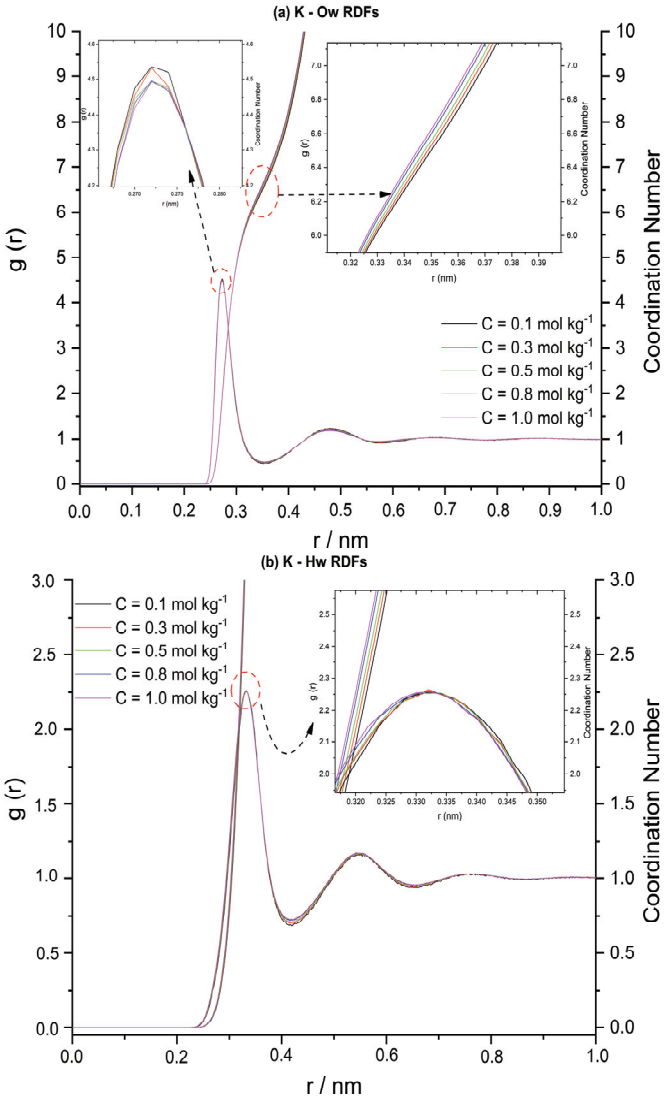

Fig. 1. $g_{K\text{-}Ow}(r)$ and $g_{K\text{-}Hw}(r)$ for potassium cation at various concentrations.

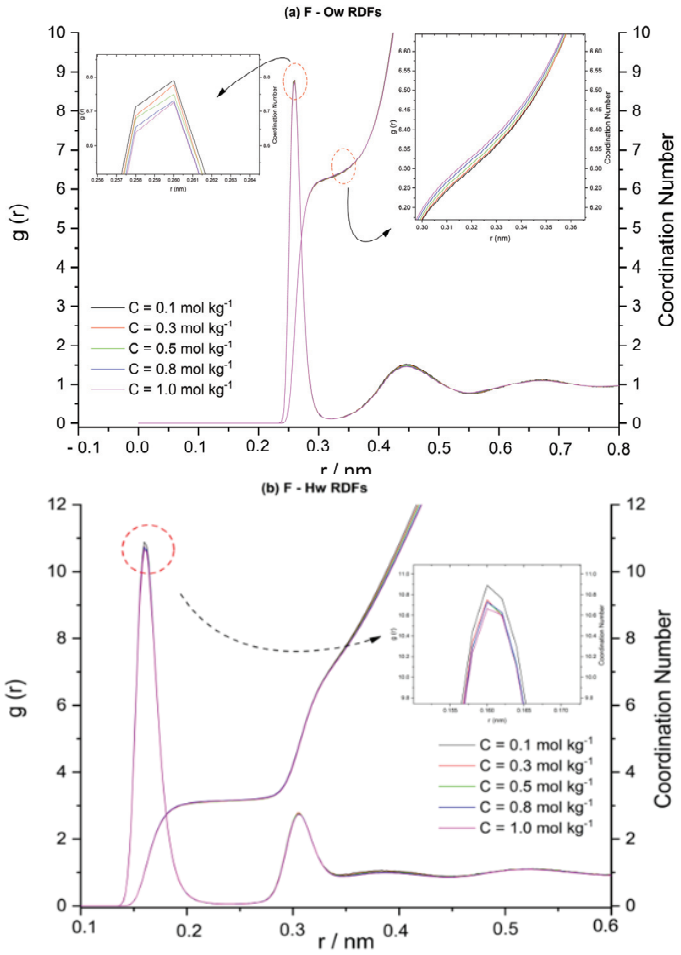

Fig. 2. $g_{\text{F-Ow}}(r)$ and $g_{\text{F-Hw}}(r)$ for fluoride anion at various concentrations.

The analysis of Fig. 2 demonstrates that the $g_{\text{F–Hw}}(r)$ function indicates the existence of two distinct peaks at distances of 0.160 and 0.305 nm, respectively. This suggests a double-layer hydration of the fluoride anion. Similarly, the $g_{\text{F–Ow}}(r)$ curve also exhibits two peaks. The first peak is observed at a distance of 0.260 nm, followed by the second one between 0.328 and 0.344 nm.

Moreover, the coordination numbers of potassium and fluoride ions increase in an almost linear with increasing concentrations. This suggests a disruption in ion-dipole interactions and an augmentation in ion–ion interactions. These coordination numbers range from 6.602 to 6.735 for K^+ and from 6.329 to 6.360 for F^-. This can be attributed to the significant difference in electronegativity between the ions, which amounts to $\Delta\eta = 3.16$ for this specific system. This difference will enable strong hydrogen bonding with H_2O molecules. Consequently,

the combined effects of $M^+\cdots H_2O$ and $M\cdots H_2O$ interactions contribute to the dissociation of KF into its fundamental ions, which leads to increased levels of hydration for F^- and K^+, especially as concentrations rise.

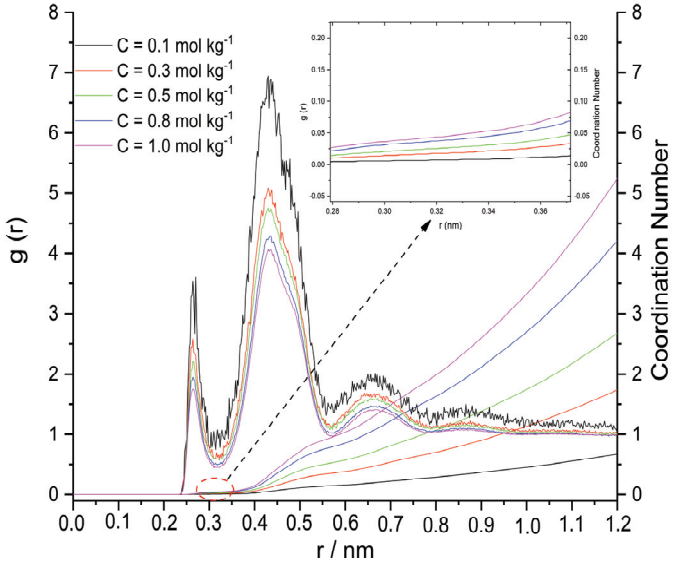

Fig. 3. Radial distribution functions $\{g_{K\text{-}F}(r)\}$ at various concentrations.

The analysis of Fig. 3 highlights the presence of four distinct groups of ion pairs. The first peak, observed at a distance of 0.264 nm, depicts ion pairs in contact (CIP). The existence of solvent-separated ion pairs (SIP) is confirmed by the second peak located at 0.428 nm. The double solvent-separated ion pairs (2SIP) are clearly identified by the third peak at a distance of 0.664 nm. Finally, free ions are represented by the last peak, which is less intense and covers a broader range of positions between 0.788 and 0.959 nm.

Moreover, the analysis of RDF variations reveals that as concentration increases, the presence of CIPs weakens, leading to a slight decrease in the coordination numbers (*CN*) of the K^+ and F^-. The strong intensity of CIPs underscores the significant binding energy between the two ions, owing to the high value of the electronegativity difference attributed to the fluoride ion.

In Fig. 4a, the increase in concentration brings forth noticeable microstructural effects in the aqueous $KF_{(aq)}$ system. The variation in the $g_{Ow\text{–}Ow}(r)$ functions demonstrates a decline in the peak intensities' maximum values. The analysis of this phenomenon signifies a considerable distortion in the structure due to intensified Ow–Ow interactions as the concentration rises. Consequently, there is a growing concentration of ions in the system, responsible for arranging water molecules regularly, thereby leading to modifications in the local structure.

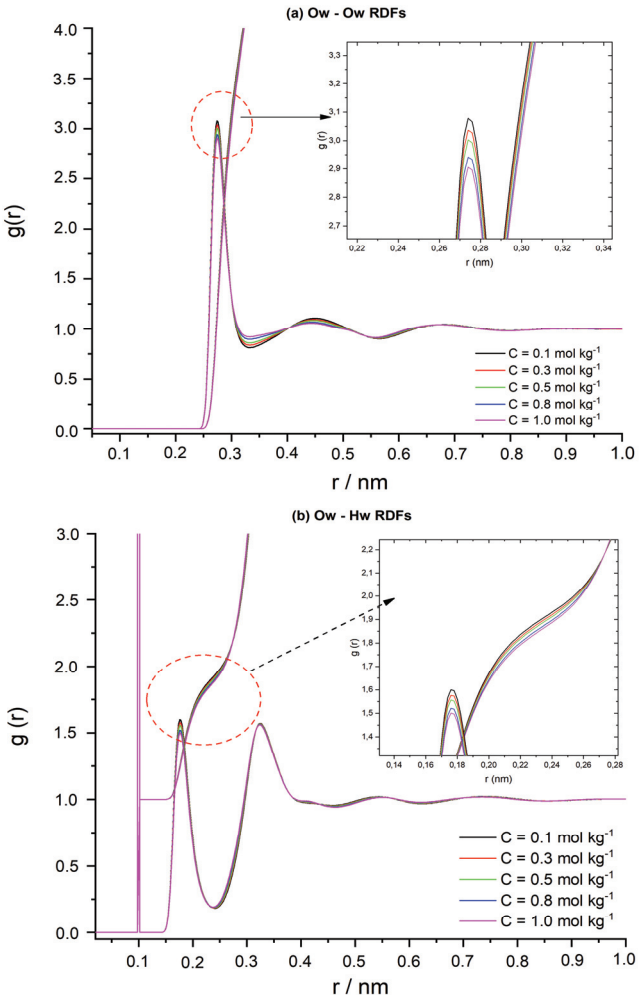

Fig. 4. $g_{\text{Ow-Ow}}(r)$ and $g_{\text{Ow-Hw}}(r)$ functions at various concentrations.

Moreover, Fig 4b illustrates the impact of concentration on the distribution of the hydrogen bond network. This is proved by the diminishing peak intensities as the concentration increases, indicating a reduction in the count of hydrogen bonds between Ow and Hw. This shift can be attributed to the strong competition between the highly electronegative fluoride anion and the oxygen atom. This competition leads to the breaking of the hydrogen bonds created by the solvent molecules (H_2O).

Dynamical and dielectric properties

Table III presents newly calculated data for the dielectric constant and self--diffusion coefficient specific to aqueous $KF_{(aq)}$ systems at various concentrat-

ions, using the molecular dynamics approach at T = 298.15 K. The analysis of Fig. 5 reveals a gradual reduction in self-diffusion coefficients as the concentration increases. Notably, this decrease is more pronounced for water molecules compared to ions, a phenomenon attributed to the stronger influence of Coulomb forces on ions.

TABLE III. Molecular dynamics results for the dielectric and dynamic properties of water molecules, ions and KF electrolyte at various concentrations

C / mol kg^{-1}	D_{KF}	D_{H_2O}	D_{K+}	D_{F^-}	Dielectric constant (ε)	Exp. data
0.1	2.5048 ±0.0252	2.5100 ±0.0239	1.8857 ±0.1246	1.1589 ±0.5037	70.2847 ± 0.4007	–
0.3	2.3891 ±0.0317	2.4040 ±0.0253	1.7974 ±0.2715	0.8693 ±0.0112	68.3135 ± 0.3450	–
0.5	2.2808 ± 0.0199	2.3093 ±0.0265	1.5111 ±0.3044	0.8416 ±0.0072	65.3158 ±0.4313	D_{H_2O} = 2.30[46]
0.8	2.1763 ±0.0700	2.2236 ±0.0638	1.4416 ±0.3613	0.7639 ±0.0338	62.1923 ± 0.1745	–
1.0	2.0115 ±0.0130	2,0507 ±0.0399	1.2499 ±0.1183	0.6842 ±0.0466	60.0358 ±0.4034	D_{H_2O} = 2.14[46] ε = 60.8[47]

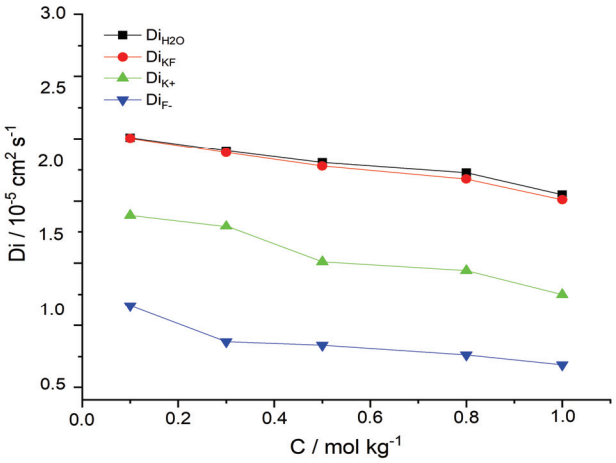

Fig. 5. Self-diffusion coefficients of both water molecules and ions within the aqueous KF system at different concentrations.

Fig. 6 illustrates that the dielectric constant values also display a decline with increasing concentration. This decrease is primarily attributed to the strength of the electric field created by the two ions (K^+ and F^-) within the aqueous solution, which weakens the polarization of the $KF_{(aq)}$ electrolytic system. Furthermore,

our results concerning the dielectric constant are in good agreement with other values from experimental data.[46,47]

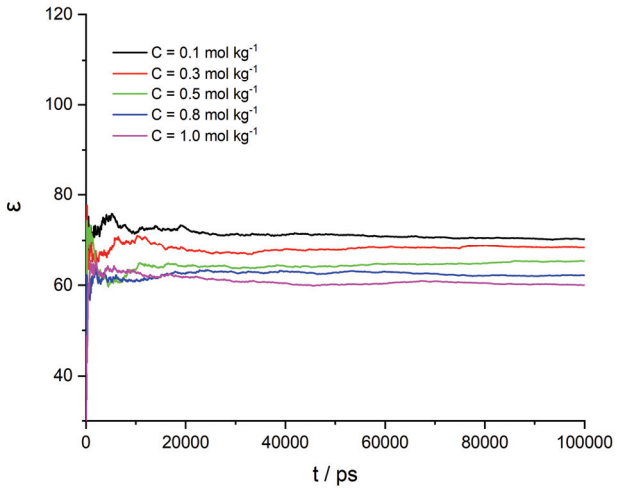

Fig. 6. Variations of the dielectric constant (ε) for the aqueous KF system as a function of simulation time at different concentrations.

CONCLUSION

In this study, we applied a molecular dynamics approach to investigate the structural, dynamical, and dielectric properties of the $KF_{(aq)}$ binary electrolyte system. The chosen method has proven highly effective for the examination of such materials in aqueous solutions. Through our molecular simulations, we gained valuable insights into the interactions between water molecules and ions (K^+, F^-), shedding light on the formation and stability of ion pairs and the intricate network of hydrogen bonds within the present aqueous electrolytic system.

Moreover, our investigation led to the determination of new simulation data regarding the self-diffusion coefficients and the dielectric constants across a broad range of concentrations, from infinite dilution to saturation, using the molecular dynamics approach. These results offer a comprehensive overview of the concentration-dependent effects on the mobility and the dielectric behaviour in potassium fluoride aqueous solutions. This knowledge significantly contributes to the understanding of the various mechanisms at play in this complex system.

Overall, this work represents a significant advancement in optimizing the use of KF electrolytes in numerous sectors, particularly within the realm of potassium-based rechargeable battery technology. The findings from our study gives the potential to enhance the efficiency and the performance of such electrolytes in industrial applications.

ИЗВОД

ИСПИТИВАЊЕ СТРУКТУРНИХ, ДИНАМИЧКИХ И ДИЕЛЕКТРИЧНИХ СВОЈСТАВА ВОДЕНИХ РАСТВОРА КАЛИЈУМ-ФЛУОРИДА РАЗЛИЧИТИХ КОНЦЕНТРАЦИЈА ПОМОЋУ МОЛЕКУЛСКЕ ДИНАМИКЕ

AYOUB LAHMIDI, SANAA RABII, ABDELKBIR ERROUGUI, SAMIR CHTITA, MHAMMED EL KOUALI и MOHAMMED TALBI

Laboratory of Analytical and Molecular Chemistry, Faculty of Sciences Ben M'Sick, Hassan II University of Casablanca, Morocco

Батерије које се заснивају на калијуму су обећавајућа алтернатива традиционалним литијум-јонским батеријама за системе за складиштење енергије услед њихове приступачности, широке доступности и хемијских карактеристика сличних литијуму. У овом раду примењене су симулације молекулске динамике да би се испитали физички феномени калијум флуорида у воденим растворима. Међуатомске интеракције су дефинисане применом OPLS-AA поља сила, док су SPC/E модел воде и јони представљени као наелектрисне Ленард–Џонсове честице. Симулације су урађене за опсег концентрација од 0,1 до 1,0 mol kg^{-1}. Резултати добијени у овом истраживању доприносе разумевању потенцијалне примене KF електролита у системима за складиштење енергије. Свеобухватно размевање утицаја концентрације KF електролита на структурне, динамичке и диелектричне особине је кључно за дизајн и оптимизацију калијум-јонских батерија, као и других електрохемијских уређаја који користе електролите засноване на KF. Ово истраживање доприноси текућим напорима усмереним ка развоју ефикасних и економски одрживих решења за складиштење енергије који превазилазе ограничења традиционалних литијум-јонских батерија.

(Примљено 6. новембра, ревидирано 23. децембра 2023, прихваћено 19. јануара 2024)

REFERENCES

1. A. Tomaszewska, Z. Chu, X. Feng, S. O'Kane, X. Liu, J. Chen, C. Ji, E. Endler, R. Li, L. Liu, Y. Li, S. Zheng, S. Vetterlein, M. Gao, J. Du, M. Parkes, M. Ouyang, M. Marinescu, G. Offer, B. Wu, *eTransportation* **1** (2019) 100011 (https://doi.org/10.1016/j.etran.2019.100011)
2. Y. Kim, W. M. Seong, A. Manthiram, *Energy Storage Mater.* **34** (2021) 250 (https://doi.org/10.1016/j.ensm.2020.09.020)
3. K. Beltrop, S. Beuker, A. Heckmann, M. Winter, T. Placke, *Energy Environ. Sci.* **10** (2017) 2090 (https://doi.org/10.1039/C7EE01535F)
4. X. Lin, J. Huang, H. Tan, J. Huang, B. Zhang, *Energy Storage Mater.* **16** (2019) 97 (https://doi.org/10.1016/j.ensm.2018.04.026)
5. H. Xu, H. Chen, C. Gao, *ACS Mater. Lett.* **3** (2021) 1221 (https://doi.org/10.1021/acsmaterialslett.1c00280)
6. R. Rajagopalan, Y. Tang, X. Ji, C. Jia, H. Wang, *Adv. Funct. Mater.* **30** (2020) 1909486 (https://doi.org/10.1002/adfm.201909486)
7. J.-Y. Hwang, S.-T. Myung, Y.-K. Sun, *Adv. Funct. Mater.* **28** (2018) 1802938 (https://doi.org/10.1002/adfm.201802938)
8. Y. Mekonnen, A. Sundararajan, A. I. Sarwat, in *Proceedings of SoutheastCon 2016*, 2016, pp. 1–6 (https://doi.org/10.1109/SECON.2016.7506639)

9. X. Zeng, M. Li, D. Abd El-Hady, W. Alshitari, A. S. Al-Bogami, J. Lu, K. Amine, *Adv. Energy Mater.* **9** (2019) 1900161 (https://doi.org/10.1002/aenm.201900161)
10. H. Vikström, S. Davidsson, M. Höök, *Appl. Energy* **110** (2013) 252 (https://doi.org/10.1016/j.apenergy.2013.04.005)
11. S. Ziemann, D. B. Müller, L. Schebek, M. Weil, *Resour. Conserv. Recycl.* **133** (2018) 76 (https://doi.org/10.1016/j.resconrec.2018.01.031)
12. R. T. Nguyen, R. G. Eggert, M. H. Severson, C. G. Anderson, *Resour. Conserv. Recycl.* **167** (2021) 105198 (https://doi.org/10.1016/j.resconrec.2020.105198)
13. G. Zubi, R. Dufo-López, M. Carvalho, G. Pasaoglu, *Renew. Sustain. Energy Rev.* **89** (2018) 292 (https://doi.org/10.1016/j.rser.2018.03.002)
14. J. Zhao, X. Zou, Y. Zhu, Y. Xu, C. Wang, *Adv. Funct. Mater.* **26** (2016) 8103 (https://doi.org/10.1002/adfm.201602248)
15. Y. Xu, C. Zhang, M. Zhou, Q. Fu, C. Zhao, M. Wu, Y. Lei, *Nat. Commun.* **9** (2018) 1720 (https://doi.org/10.1038/s41467-018-04190-z)
16. S. Zhang, Y. Liu, Q. Fan, C. Zhang, T. Zhou, K. Kalantar-Zadeh, Z. Guo, *Energy Environ. Sci.* **14** (2021) 4177 (https://doi.org/10.1039/D1EE00531F)
17. L. Jiang, Y. Lu, C. Zhao, L. Liu, J. Zhang, Q. Zhang, X. Shen, J. Zhao, X. Yu, H. Li, X. Huang, L. Chen, Y.-S. Hu, *Nat. Energy* **4** (2019) 495 (https://doi.org/10.1038/s41560-019-0388-0)
18. K. Kubota, M. Dahbi, T. Hosaka, S. Kumakura, S. Komaba, *Chem. Rec.* **18** (2018) 459 (https://doi.org/10.1002/tcr.201700057)
19. J. C. Pramudita, D. Sehrawat, D. Goonetilleke, N. Sharma, *Adv. Energy Mater.* **7** (2017) 1602911 (https://doi.org/10.1002/aenm.201602911)
20. Z. Jian, Y. Liang, I. A. Rodríguez-Pérez, Y. Yao, X. Ji, *Electrochem. Commun.* **71** (2016) 5 (https://doi.org/10.1016/j.elecom.2016.07.011)
21. M. Sajjad, F. Cheng, W. Lu, *RSC Adv.* **11** (2021) 25450 (https://doi.org/10.1039/D1RA02445K)
22. X. Lu, M. E. Bowden, V. L. Sprenkle, J. Liu, *Adv. Mater.* **27** (2015) 5915 (https://doi.org/10.1002/adma.201502343)
23. S. Liu, L. Kang, J. Henzie, J. Zhang, J. Ha, M. A. Amin, M. S. A. Hossain, S. C. Jun, Y. Yamauchi, *ACS Nano* **15** (2021) 18931 (https://doi.org/10.1021/acsnano.1c08428)
24. Y.-S. Xu, S.-Y. Duan, Y.-G. Sun, D.-S. Bin, X.-S. Tao, D. Zhang, Y. Liu, A.-M. Cao, L.--J. Wan, *J. Mater. Chem., A* **7** (2019) 4334 (https://doi.org/10.1039/C8TA10953B)
25. Y. Wu, Y. Sun, Y. Tong, X. Liu, J. Zheng, D. Han, H. Li, L. Niu, *Energy Storage Mater.* **41** (2021) 108 (https://doi.org/10.1016/j.ensm.2021.05.045)
26. A. Errougui, M. Talbi, M. Kouali, *E3S Web Confer.* **297** (2021) 01009 (https://doi.org/10.1051/e3sconf/202129701009)
27. T. Noël, Y. Cao, G. Laudadio, *Acc. Chem. Res.* **52** (2019) 2858 (https://doi.org/10.1021/acs.accounts.9b00412)
28. A. Errougui, M. Talbi, M. El Kouali, *Egypt. J. Chem.* **65** (2022) 1 (https://doi.org/10.21608/ejchem.2021.67302.3453)
29. A. Errougui, A. Lahmidi, S. Chtita, M. El Kouali, M. Talbi, *J. Solut. Chem.* **52** (2023) 176 (https://doi.org/10.1007/s10953-022-01222-7)
30. G. A. Kaminski, R. A. Friesner, J. Tirado-Rives, W. L. Jorgensen, *J. Phys. Chem., B* **105** (2001) 6474 (https://doi.org/10.1021/jp003919d)

31. M. J. Abraham, T. Murtola, R. Schulz, S. Páll, J. C. Smith, B. Hess, E. Lindahl, *SoftwareX* **1**–**2** (2015) 19 (https://doi.org/10.1016/j.softx.2015.06.001)
32. B. Hess, C. Kutzner, D. Van Der Spoel, E. Lindahl, *J. Chem. Theory Comput.* **4** (2008) 435 (https://doi.org/10.1021/ct700301q)
33. M. Parrinello, A. Rahman, *J. Appl. Phys.* **52** (1981) 7182 (https://doi.org/10.1063/1.328693)
34. S. Nosé, *Mol. Phys.* **52** (1984) 255 (https://doi.org/10.1080/00268978400101201)
35. W. G. Hoover, *Phys. Rev., A* **31** (1985) 1695 (https://doi.org/10.1103/PhysRevA.31.1695)
36. H. J. C. Berendsen, J. R. Grigera, T. P. Straatsma, *J. Phys. Chem.* **91** (1987) 6269 (https://doi.org/10.1021/j100308a038)
37. S. I. Sandler, & J. K. Wheatley, *Chem. Phys. Lett.* **10** (1971) 375 (https://doi.org/10.1016/0009-2614(71)80313-5)
38. C. J. Fennell, A. Bizjak, V. Vlachy, K. A. Dill, *J. Phys. Chem., B* **113** (2009) 6782 (https://doi.org/10.1021/jp809782z)
39. J. Zielkiewicz, *J. Chem. Phys.* **123** (2005) 104501 (https://doi.org/10.1063/1.2018637)
40. S. Reiser, S. Deublein, J. Vrabec, H. Hasse, *J. Chem. Phys.* **140** (2014) 044504 (https://doi.org/10.1063/1.4858392)
41. *Experimental Determination of Partial and Environmental Structure Functions in Non-crystalline Systems — Fundamental Aspects*. in *Anomalous X-Ray Scattering for Material Characterization: Atomic-Scale Structure Determination*, Y. Waseda, Ed., Springer, Berlin, 2002, pp. 9–20 (https://doi.org/10.1007/3-540-46008-X_2)
42. M. Guo, W. Wang, H. Lu, *Fluid Phase Equilib.* **60** (1990) 37 (https://doi.org/10.1016/0378-3812(90)85041-8)
43. X. Zhang, X. Liu, M. He, Y. Zhang, Y. Sun, X. Lu, *Fluid Phase Equilib.* **518** (2020) 112625 (https://doi.org/10.1016/j.fluid.2020.112625)
44. S. Deublein, J. Vrabec, H. Hasse, *J. Chem. Phys.* **136** (2012) 084501 (https://doi.org/10.1063/1.3687238)
45. Y. Laudernet, T. Cartailler, P. Turq, M. Ferrario, *J. Phys. Chem., B* **107** (2003) 2354 (https://doi.org/10.1021/jp0223814)
46. D. W. McCall, D. C. Douglass, *J. Phys. Chem.* **69** (1965) 2001 (https://doi.org/10.1021/j100890a034)
47. F. E. Harris, C. T. O'Konski, *J. Phys. Chem.* **61** (1957) 310 (https://doi.org/10.1021/j150549a009).